Structure and Superconductivity of FeSe$_{1-x}$ and FeTe$_{1-y}$Se$_y$ Crystals: Dependence on the Synthesis Methods, Starting Composition, and Growth Conditions

D.J. Gawryluk[a,*], J. Fink-Finowicki[a], A. Wiśniewski[a], R. Puźniak[a], V. Domukhovski[a],
R. Diduszko[a,b] and M. Berkowski[a]

[a]Institute of Physics, Polish Academy of Sciences, al. Lotników 32/46, PL-02-668 Warsaw, Poland

[b]Institute of Electronic Materials Technology, Wólczyńska 133, PL-01-919 Warsaw, Poland

Syntheses of superconducting iron chalcogenides FeSe$_{1-x}$ ($x = 0$–0.15) and FeTe$_{1-y}$Se$_y$ ($y = 0.3$–0.55) were performed. Superconducting phase of iron selenide was obtained by the solid-state reaction and from liquid phase. The highest values of critical temperature ($T_c = 8.2$–8.7 K) exhibit FeSe$_{1-x}$ obtained by the crystallization from a melt with excess of iron less than 1 mol%. The samples from a melt contain up to 78% of tetragonal phase, as estimated by the X-ray diffraction. Lattice parameters and unit cell volume for the samples exhibiting highest T_c and sharpest transition to superconducting state are limited to narrow range, with c/a ratio close to 1.469. The samples with excess of selenium contain higher amount of hexagonal phase than stoichiometric one. Superconducting single-crystalline samples of FeTe$_{1-y}$Se$_y$ (up to 100% of tetragonal phase) were obtained using Bridgman's method. When y value increases, the volume of unit cell decreases. The critical temperature T_c changes from ≈ 11.5 K for $y \approx 0.3$ to ≈ 14.7 K for $y \approx 0.5$.

PACS numbers: 61.05.cp, 74.25.Ha, 74.62.Bf, 74.70.Xa, 81.10.Fq

1. Introduction

The discovery of superconductivity in LaFeAsO$_{1-x}$F$_x$ ($T_c = 26$ K at ambient pressure) [1] has generated intensive research of the pnictogen–iron systems with various chemical substitutions. There is common feature of all iron-based superconductors — layered structure with layers of iron coordinated by arsenic or phosphorus. The iron-based superconductor with the simplest crystallographic structure is tetragonal (space group $P4/nmm$), non-stoichiometric iron selenide FeSe$_{1-x}$ ($T_c \approx 8.5$ K). Critical temperature for this compound increases even up to ≈ 37 K under high pressure [2–5]. Simple chemical formula, as well as the less toxicity than arsenic compounds, are the reasons to consider the FeSe as a model system for investigations of mechanism of superconductivity and relation between structural, magnetic, and superconducting properties in iron-based compounds family. Moreover, great interest attracts coexistence of magnetism and superconductivity in this group of materials.

The first report about superconducting FeSe$_{1-x}$ described solid state reaction technique of pressed iron and selenium powders in quartz tube [6]. Starting compositions for synthesis of superconducting iron selenide in solid state reaction were in a wide range of $x = $

* corresponding author; e-mail: `gawryluk@ifpan.edu.pl`

0.28–0.02 [7, 8] while range of heating temperatures was 450–750 °C. Synthesis at lower temperatures enlarges the probability of an occurrence of elementary selenium precipitations but on the other hand reduces silicates impurities formation.

Significant progress in synthesis of iron selenide superconductor was achieved by McQueen et al. [9], who proposed the crystallization from a melt at 1075 °C. The authors reported that tetragonal phase is stable in the broad temperature range 300–450 °C. Therefore, the key factor is annealing of the material at the temperature from this range of stability prior to rapid cooling. Syntheses of non-stoichiometric iron selenides were performed from freshly cleaned Fe pieces and Se ingots in quartz ampoules with carbon inside. This was the first paper reporting narrow range of x value: $x = 0.01$–0.03 in which the material shows the superconductivity. Report by Williams et al. [10] was the next work which confirmed near stoichiometric composition as a correct one for the superconducting iron selenides. Only FeSe$_{0.99}$ contains mainly tetragonal phase (without iron precipitations as well as without presence of hexagonal phase, earlier defined as Fe$_7$Se$_8$). Magnetic measurements showed that sample in which the volume of tetragonal (superconducting) phase is large enough, exhibits identical critical temperature as that one of pure tetragonal sample. Only the width of transition differs for both samples as well as

paramagnetic background, which is closely linked with excess of iron. The above statements are correct when samples are synthesized with care about lack of contact with oxygen and moisture. It is very important to start synthesis with really pure substrates, which is impossible to achieve when one starts it from powders.

Various chemical substitutions to Fe–Se system were done. Iron was substituted by Na, Al, Ti, V, Cr, Mn, Co, Ni, Cu, Ga, In, Ba, Sm, as well as selenium was substituted by S and Te [11–14]. However, it is difficult to obtain large single crystals of superconducting FeSe. Particularly interesting is isostructural, pseudobinary system Fe–Se–Te, which relatively easy crystallizes and is characterized by higher T_c than that of Fe–Se system. Hence, it is ideal material for various physical investigations. In order to obtain large single crystals of FeTe$_{1-y}$Se$_y$ system, Bridgman's method has been used. So far single crystals have shown bulk superconductivity in narrow range of composition for $y \approx 0.5$ [15–17]. Moreover, single crystals for $y = 0.5$ exhibit coexistence of two tetragonal phases, which results in a reflex splitting at diffraction pattern. Presence of two different tetragonal phases for polycrystalline materials has been reported for the substitution range $0.7 < y < 0.85$ [11, 18]. One phase is stable for $y = 0.85–1$ ($T_c \approx 8–10$ K), while the other one is stable for $y = 0–0.7$ ($T_c \approx 15$ K). Additionally, hexagonal FeSe (space group $P6_3/mmc$) occurs in the regions with low concentration of tellurium [11, 15, 18].

2. Experimental

For the syntheses of superconducting iron chalcogenides systems FeSe$_{1-x}$ with starting composition $x = 0$–0.15 and FeTe$_{1-y}$Se$_y$ with $y = 0.3$–0.55, the following chemicals: FeSe, Fe, Se, and Te 4N purity were used as starting materials. All of the materials were weighed, mixed and stored in glove box in argon atmosphere. Superconducting phase of iron selenide was obtained by the solid state reaction or by melting of the previously synthesized materials.

The solid state reactions were performed in evacuated and sealed quartz ampoules. Hereafter we call these samples the A series. Syntheses were done for 24 to 48 h at temperatures ranging from 700 to 750 °C. The obtained sinters were regrounded and after that were calcinated again at the identical temperature. After synthesis the temperature was reduced to 340 °C with the rate of 180 °C/h. At this temperature ampoules were held for at least 24 h and then the ampoules were pulled out and were cooled down in water.

Crystallization of iron selenide from a melt was performed in evacuated sealed double wall quartz ampoules (B series). All syntheses and crystallization processes were done in vertical furnace. After 24–48 h of the synthesis the fused materials were maintained at 1085 °C. This temperature was held by the next 24 h. Ampoules with samples were cooled down to 1025 °C with the rate of 3 °C/h, subsequently to 340 °C with the rate

of 30–40 °C/h. The samples were kept at 340 °C for 24 h prior to quick cooling down in water bath.

Crystallization process of FeTe$_{1-y}$Se$_y$ for $y = 0.55$–0.30 was performed using Bridgman's method (T series). Double walled evacuated sealed quartz ampoules with substrates were placed in a furnace with the vertical gradient of temperature equal to 1.2 °C/mm. These samples were synthesized in the same conditions as those for FeSe$_{1-x}$ and next the temperature was risen to 950 °C. After melting of components the temperature was held for 12 h, then samples were cooled down to 700 °C with step of 1–3 °C/h and subsequently to 350 °C with the rate of 15 °C/h, and finally cooled down to the room temperature with the furnace.

Magnetic measurements of all the samples were performed with a physical property measurement system (PPMS) of Quantum Design. The measurements of DC magnetization (using zero-field-cooling (ZFC) and field--cooling (FC) procedures in $H = 10$ Oe) and AC susceptibility (field amplitude 1 and 10 Oe, frequencies 1 and 10 kHz) allowed to determine the critical temperature T_c and the width of the transition, as well as to estimate volume fraction of the superconducting phase.

Phase analysis and structural refinement of the crystals was performed by X-ray powder diffraction using Ni--filtered Cu K_α radiation with a Siemens D5000 diffractometer. Data were collected in the angle range $20° < 2\theta < 100°$ with a step of $0.02°$ and averaging time of 10 s/step. The powder diffraction patterns were analyzed by the Rietveld refinement method using DBWS--9807 program [19].

3. Results and discussion

The temperature dependences of zero field cooled and field cooled DC susceptibility for FeSe$_{1-x}$ samples are shown in Fig. 1. shapes (it implicates different values of
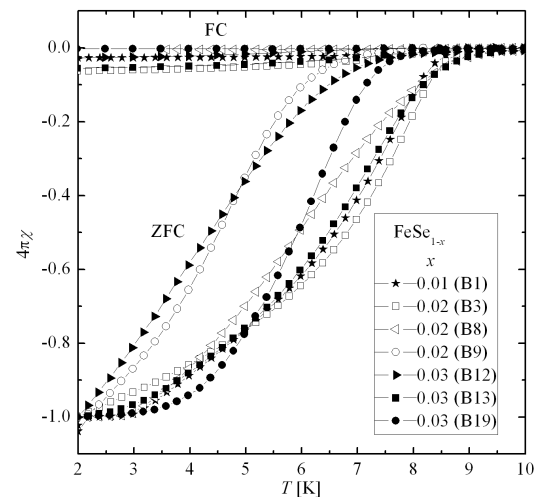

Fig. 1. DC susceptibility for FeSe$_{1-x}$ samples determined in external magnetic field of 10 Oe in zero field cooling and field cooling mode.
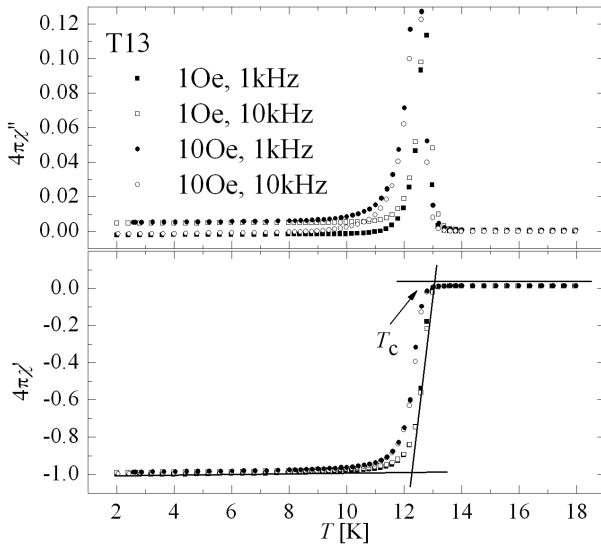
Fig. 2. Real (bottom) and imaginary (top) part of AC susceptibility for $FeTe_{0.65}Se_{0.35}$ sample measured in 1 and 10 Oe of AC field with 1 and 10 kHz.

demagnetization coefficient), so The samples had different values of magnetic susceptibility for all of the samples were normalized in borders $(0, -1)$. Broad width of the transition to superconducting state could be linked with deviation from nominal composition in some areas of the samples. Low absolute value of FC magnetization is due to strong pinning of vortices and indicates a presence of many defects in the sample. The highest values of critical temperature ($T_c = 8.2$–8.7 K) exhibit polycrystalline samples of $FeSe_{1-x}$ for $x = 0$–0.03, obtained by the crystallization from liquid phase. The best superconducting parameters are exhibited by iron selenides with iron excess smaller than 1 mol%. For the samples with larger iron excess, paramagnetic background, increasing with increasing iron concentration, is observed.

Temperature dependences of real and imaginary part of AC susceptibility for $FeTe_{0.65}Se_{0.35}$ sample are shown in Fig. 2. Sharp transition to the superconducting state confirms really good homogeneity. The superconducting response decreases only very slightly with increasing amplitude of AC field suggesting the lack of weak links in the sample.

Powder diffraction patterns for selected $FeSe_{1-x}$ and $FeTe_{0.65}Se_{0.35}$ samples are shown in Fig. 3. The crystal data and the values of critical temperature for selected samples are collected in Table. The samples obtained by the solid state reaction, as well as by the melting, contain hexagonal and tetragonal phases of iron selenide. In the samples which were synthesized without melting the traces of iron oxide (mainly Fe_3O_4), iron, and elementary selenium appear. The fraction of tetragonal phase in these samples varies from 52 to 58%. Only the samples that were sintered at 750 °C contain up to 96% of tetragonal phase. In the samples crystallized from melt, the content of tetragonal phase varies from 68% to 78%.

The samples with higher concentration of selenium contain higher amount of hexagonal phase, characteristic for Fe_7Se_8. Lattice parameters and volume of the unit cell for the samples obtained by various methods vary in a broad range. Lattice parameters for the samples with the highest T_c and the sharpest transition to superconducting state are observed to take values in the narrow range around $a = 3.767 \pm 0.001$ and $c = 5.533 \pm 0.002$.
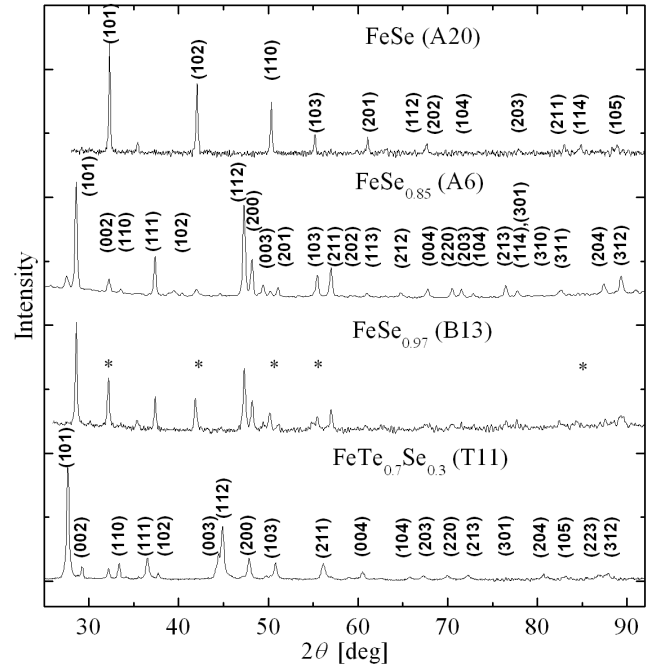

Fig. 3. X-ray powder diffraction patterns of: A20-FeSe (100% $P6_3/mmc$), A6-FeSe$_{0.85}$ (96% $P4/nmm$), B13-FeSe$_{0.97}$ (78% $P4/nmm$+22% $P6_3/mmc$, marked with an asterisk), T11-FeTe$_{0.7}$Se$_{0.3}$ (up to 100% $P4/nmm$) samples.

Superconducting samples of $FeTe_{1-y}Se_y$ obtained in crystallization process contain up to 100% of tetragonal phase. The obtained crystallites (mass up to 7 g) exhibit natural cleavage plane c. Full width at half maximum (FWHM) of (004) reflex measured on the best single crystals is equal to $\Delta\omega = 6'$. Strong texture of crystalline powder obtained by grinding of the monocrystalline samples render difficult to correct powder refinement analyses. When vertical gradient of temperature in the furnace is too small, disoriented small size blocks are formed even in a cone part of the ampoule. An increase of the vertical gradient of temperature from 0.5 °C/mm to ≈ 1.2 °C/mm leads to a decrease of linear speed of crystal growth down to ≈ 1.6–2 mm/h.

TABLE

Crystal data and values of critical temperature for selected samples of $FeSe_{1-x}$ (A and B series) and $FeTe_{1-y}Se_y$ (T series).

No.	x or y	Space group	a [Å]	c [Å]	c/a	V [Å^3]	% of tetragonal phase	T_c [K]	ΔT_c [K]
A6	0.15	$P4/nmm$	3.772	5.530	1.466	78.67	96		
A20	0	$P6_3/mmc$	3.686	5.893	1.599	69.32	0	–	–
B1	0.01		3.766	5.528	1.468	78.41	61	8.5	5.5
B3	0.02		3.762	5.536	1.472	78.36	65	8.5	6.5
B8	0		3.768	5.532	1.468	78.52	67	8.7	5.8
B9	0.02	$P4/nmm$	3.768	5.529	1.467	78.51	73	6.3	4.3
B12	0.03		3.767	5.533	1.469	78.52	71	6.7	4.7
B13	0.03		3.763	5.540	1.472	78.44	78	8.5	4.9
B19	0.03		3.767	5.529	1.468	78.46	72	7.5	3.5
T2	0.5		3.778	6.084	1.610	86.86	90	14.7	1.7
T5	0.3	$P4/nmm$	3.799	6.103	1.606	88.08	91	12.9	5.9
T11	0.3		3.802	6.115	1.608	88.40	100	11.5	4.2
T13	0.35		3.806	6.092	1.601	88.25	100	12.9	0.6

4. Conclusions

The samples obtained in solid state reaction exhibit worse superconducting properties than the others despite of larger content of tetragonal phase (T_c lower than 7.5 K). The samples exhibit wider transition to superconducting state as well as their paramagnetic background is higher. The samples of $FeSe_{1-x}$ with $x = 0$–0.03, obtained by the crystallization from liquid phase, exhibit the highest T_c up to 8.7 K. The width of the transition is rather wide and equals to 3.5–6.5 K. In order to obtain samples which exhibit the best superconducting properties it is required to protect substrates from oxygen contact and to use well adjusted temperature conditions as well as to start synthesis from composition near stoichiometric one (iron excess below 1 mol%). The highest values of critical temperature ($T_c = 14.3$–14.7 K) with sharp transition to the superconducting state (width of about 1.7 K) are obtained for $FeTe_{1-y}Se_y$ with $y \approx 0.5$. Critical temperature T_c decreases even to ≈ 11.5 K for $y < 0.3$. For all of the obtained samples, when y value increases, the volume of unit cell decreases.

References

[1] Y. Kamihara, T. Watanabe, M. Hirano, H. Hosono, *J. Am. Chem. Soc.* **130**, 3296 (2008).

[2] Y. Mizuguchi, F. Tomioka, S. Tsuda, T. Yamaguchi, Y. Takano, *Appl. Phys. Lett.* **93**, 152505 (2008).

[3] S. Margadonna, Y. Takabayashi, Y. Ohishi, Y. Mizuguchi, Y. Takano, T. Kagayama, T. Nakagawa, M. Takata, K. Prassides, *Phys. Rev. B* **80**, 064506 (2009).

[4] G. Garbarino, A. Sow, P. Lejay, A. Sulpice, P. Toulemonde, M. Mezouar, M. Nunez-Regueiro, *Europhys. Lett.* **86**, 27001 (2009).

[5] S. Medvedev, T.M. McQueen, I. Trojan, T. Palasyuk, M.I. Eremets, R.J. Cava, S. Naghavi, F. Casper, V. Ksenofontov, G. Wortmann, C. Felser, *Nature Mater.* **8**, 630 (2009).

[6] F.-C. Hsu, J.-Y. Luo, K.-W. Yeh, T.-K. Chen, T.-W. Huang, P.M. Wu, Y.-C. Lee, Y.-L. Huang, Y.-Y. Chu, D.-C. Yan, M.-K. Wu, *Proc. Natl. Acad. Sci.* **105**, 14262 (2008).

[7] D. Phelan, J.N. Millican, E.L. Thomas, J.B. Leao, Y. Qiu, R. Paul, *Phys. Rev. B* **79**, 014519 (2009).

[8] J. Janaki, T. Geetha Kumary, Awadhesh Mani, S. Kalavathi, G.V.R. Reddy, G.V. Narasimha Rao, A. Bharathi, *J. Alloys Comp.* **486**, 37 (2009).

[9] T.M. McQueen, Q. Huang, V. Ksenofontov, C. Felser, Q. Xu, H. Zandbergen, Y.S. Hor, J. Allred, A.J. Williams, D. Qu, J. Checkelsky, N.P. Ong, R.J. Cava, *Phys. Rev. B* **79**, 014522 (2009).

[10] A.J. Williams, T.M. McQueen, R.J. Cava, *Solid State Commun.* **149**, 1507 (2009).

[11] Y. Mizuguchi, F. Tomioka, S. Tsuda, T. Yamaguchi, Y. Takano, *J. Phys. Soc. Jpn.* **78**, 074712 (2009).

[12] Z.Q. Liu, A.H. Fang, F.Q. Huang, M.H. Jiang, arXiv:0808.1784v1 (2008).

[13] T.-W. Huang, T.-K. Chen, K.-W. Yeh, C.-T. Ke, C.L. Chen, Y.-L. Huang, F.-C. Hsu, M.-K. Wu, P.M. Wu, M. Avdeev, A.J. Studer, arXiv:0907.4001v1 (2009).

[14] M.K. Wu, F.C. Hsu, K.W. Yeh, T.W. Huang, J.Y. Luo, M.J. Wang, H.H. Chang, T.K. Chen, S.M. Rao, B.H. Mok, C.L. Chen, Y.L. Huang, C.T. Ke, P.M. Wu, A.M. Chang, C.T. Wu, T.P. Perng, *Physica C* **469**, 340 (2009).

[15] B.C. Sales, A.S. Sefat, M.A. McGuire, R.Y. Jin, D. Mandrus, Y. Mozharivskyj, *Phys. Rev. B* **79**, 094521 (2009).

[16] R. Khasanov, M. Bendele, A. Amato, P. Babke-vich, A.T. Boothroyd, A. Cervellino, K. Conder, S.N. Gvasaliya, H. Keller, H.-H. Klauss, H. Luetkens, E. Pomjakushina, B. Roessli, *Phys. Rev. B* **80**, 140511 (2009).

[17] M.D. Lumsden, A.D. Christianson, E.A. Gore-mychkin, S.E. Nagler, H.A. Mook, M.B. Stone, D.L. Abernathy, T. Guidi, G.J. MacDougall, C. de la Cruz, A.S. Sefat, M.A. McGuire, B.C. Sales, D. Mandrus, arXiv:0907.2417v1 (2009).

[18] M.H. Fang, H.M. Pham, B. Qian, T.J. Liu, E.K. Vehstedt, Y. Liu, L. Spinu, Z.Q. Mao, *Phys. Rev. B* **78**, 224503 (2008).

[19] R.A. Young, A.C. Larson, C.O. Paiva-Santos, *DBWS- -9807 Program for Rietveld Analysis*, School of Physics, Georgia Institute of Technology, Atlanta 1998.